The use of difference spectra with a filtered rolling average background in mobile gamma spectrometry measurements

A.J. Cresswell*, D.C.W. Sanderson

Scottish Universities Environmental Research Centre, Rankine Avenue, Scottish Enterprise Technology Park, East Kilbride, Glasgow G75 0QF, UK

Abstract

The use of difference spectra, with a filtering of a rolling average background, as a variation of the more common rainbow plots to aid in the visual identification of radiation anomalies in mobile gamma spectrometry systems is presented. This method requires minimal assumptions about the radiation environment, and is not computationally intensive. Some case studies are presented to illustrate the method. It is shown that difference spectra produced in this manner can improve signal to background, estimate shielding or mass depth using scattered spectral components, and locate point sources. This approach could be a useful addition to the methods available for locating point sources and mapping dispersed activity in real time. Further possible developments of the procedure utilising more intelligent filters and spatial averaging of the background are identified.

Keywords: Gamma spectrometry; Airborne; Mobile; Processing; Mapping; Real-time

* Corresponding author: Tel: +44 1355 270107.

E-mail address: a.cresswell@suerc.gla.ac.uk

1. Introduction

The use of mobile platforms to record gamma ray spectra is a common method for rapid determination of the distribution of radionuclides in the environment, both for mapping dispersed activity [1-4] and locating point sources [2, 5]. Typically such systems consist of sensitive gamma ray detectors mounted in either a low flying aircraft or four wheel drive vehicle, though other platforms are also sometimes used (for example, hovercraft [6]). For airborne survey, the detector typically consists of 16 litres, or more, of NaI(Tl) scintillator, often supplemented by one or more germanium semiconductor detectors. Equipment consisting of spectrometry systems, radar altimeter to measure vertical height of the detector above ground, GPS receiver to record the positions of each measurement and data logging computer is used to record and analyse a series of gamma-ray spectra tagged with positional and ground clearance data. Similar equipment is used for ground based systems, though usually with a much smaller detector.

The need for systems able to locate point sources is well recognised. Several incidents have occurred where mobile systems using gamma spectrometry equipment have been deployed to locate such sources. These have included locating an Athena missile carrying two ^{57}Co sources in 1970 [7], debris from the nuclear powered Cosmos-954 satellite that re-entered the atmosphere over Canada in 1978 [8, 9] and the 1987 accident at Goiânia in Brazil [10].

More recently, a series of exercises have been conducted that included searches for hidden sources using mobile gamma spectrometry systems. In 1995, the Resume 95

exercise in Finland with 10 airborne and 7 vehicular teams included a search of a small area in which sources of ^{60}Co, ^{137}Cs, ^{192}Ir and ^{99}Tc with a range of activities and shielding had been hidden [11]. A further Resume 99 exercise in Sweden in 1999 involved 10 carborne systems [12] with ^{137}Cs and ^{99m}Tc sources hidden near the end of a 200 km long route driven by all teams. The 2001 Barents Rescue Exercise in Sweden included a gamma source search exercise involving 7 airborne and 11 carborne systems, with a total of 44 different sources of ^{241}Am, ^{60}Co, ^{137}Cs, ^{131}I, ^{192}Ir, ^{99}Mo and ^{226}Ra placed in the search area [13, 14]. The results from these exercises demonstrated that about 50% of the sources used were located, with virtually all teams locating strong unshielded sources and very few teams locating small or well shielded sources.

Several methods have been developed to aid in identifying sources in response to such incidents, many of them have been practiced at international exercises like those mentioned above. Early source searches often used simple total counts or dose rate measurements, or standard processing techniques with minimal modification to identify sources after the survey was completed. For example, at both the RESUME 1995 [11] and Barents Rescue [13, 14] exercises, airborne survey teams presented source location and identities to the organisers within one hour of landing, allowing standard processing and follow-up data analysis of suspected sources.

Methods to provide real-time indicators to the operators have also been developed, allowing much faster reporting of potential sources. These can use simple count rates, either for the whole spectrum or specific spectral windows corresponding to the full energy peaks for radionuclides of interest. However, processing of the spectra to

remove backgrounds and interferences produce more reliable and sensitive means of providing real-time indicators for operators.

Standard spectral windows processing, where the count rates in predefined regions of interest are analysed by the subtraction of a fixed detector background followed by stripping out of interferences from other peaks and an altitude correction and calibration [1-3, 15], has been widely used in real-time applications [16-18].

However, the windows method requires a prior knowledge of the isotope(s) of interest so that a suitable stripping matrix can be produced, and suitable backgrounds need to be measured. If these processing parameters are not known this method can be used with working values, although this may reduce the precision with which sources can be identified and a source producing gamma rays that are not included in the windows used may not register.

Another approach that can be used in real time analysis to locate sources exploits the fact that anthropogenic radionuclides tend to produce gamma rays at relatively low energies (below 1500 keV), whereas naturally occurring radionuclides also produce higher energy gamma rays. A ratio of the count rates in low energy to high energy regions of the spectrum can thus identify the presence of anthropogenic activity. This approach was used to locate fragments of the Cosmos 954 satellite [9], and a similar approach using the ratio of count rates in lower energy windows was used in the Resume 95 exercise to locate a ^{192}Ir source [19].

The statistical analysis of the gross count rate in windows centred on a peak associated with the radionuclide of interest has also been used for real-time source detection [20, 21]. The approach assumes that the majority of spectra measured during a source search only contains the natural background, and uses this continuous flow of spectra to apply statistical methods to determine if a source is present in the field of view of the detector.

Over recent years, the use of graphical means of displaying real-time information to the operators of such systems has become common. In particular many systems use displays that are variously called “waterfall” or “rainbow” plots [5, 16-18, 22]. These plots show the most recent spectrum recorded, colour-coded by the number of counts per channel, with a ‘waterfall’ plot (with the x-axis being channel number, the y-axis measurement number and the point colour indicating the counts per channel) showing a visual record of recent measurements. Such plots allow a trained operator to monitor the performance of the detector system and notice any large variations in the radiation environment, such as discontinuities caused by boundaries between different environments or localised point sources.

For locating point sources, the rainbow plot is particularly useful as it allows the operator to immediately see if they are in the vicinity of such a source. However, a source may be easily missed if it is small compared to the local background, shielded or distant from the detector. A variation on the standard rainbow plot is the subtraction of a representative local background from measured spectra, generating difference spectra. Such difference spectra enhance the ability of operators to identify and locate sources in real time by highlighting sudden changes in the radiation

environment. The resulting difference spectra are then displayed on a rainbow plot, in exactly the same way as gross spectra are routinely displayed.

A rolling background of the average of the most recent spectra is often used. A recognised draw back of this approach is that immediately after a source the background spectra include signals associated with the source, producing negative difference spectra. Likewise, when crossing water-land boundaries this approach can produce large positive difference spectra. Alternatively, a fixed background spectrum can be subtracted. This approach requires sufficient data to have already been collected in the area for such a representative spectrum to be determined. And, it is highly unlikely that such a spectrum would be truly representative of the radiation environment over large areas.

A modification to the rolling background approach, which reduces the effects produced by boundaries and passing sources, is described here. This uses a filter to determine whether the current spectrum is to be included in the background. This retains the local nature of the rolling background while excluding data that vary significantly from it, such as those that are collected over sources or water.

2. Method

A difference spectrum is determined by simply subtracting a local background spectrum, in this case a rolling average background, from the measured spectrum. One or more filters are then applied to determine whether or not the current spectrum should be included in the rolling average background.

First, any spectra that fall outside a defined ground clearance range appropriate for the survey are not included in the background. By keeping this range of ground clearances narrow the need for any altitude dependence in the filter is removed. Data with total count rates less than twice the background from the detector, aircraft and cosmic ray components are rejected from inclusion in the background, as these are most likely to be recorded over open water.

The simplest filter to apply at this point would be a comparison of the measured spectrum to gross count rate values within specified spectral windows, with spectra where the count rates exceed these values not included in the rolling average background. Though simple, this approach has some noticeable weaknesses. The levels at which the filter is activated will need to be matched to the local environment. In an area where ambient radiation levels are relatively high a low threshold will result in the filter excluding too many spectra from the local background. Conversely, a higher threshold will include spectra in the rolling average background that differ significantly from the local background where radiation levels are lower. Setting the appropriate levels for such a filter will require some prior knowledge of the survey area. And, even within a single survey the local background radiation levels can be sufficiently variable to make a single set of absolute values inappropriate for the whole area. With the exception of the low level filter to identify data recorded over water, an approach has been adopted here that filters the spectra according to the significance of the variations between the measured spectrum and the rolling average background.

For the measurements that pass the first filters, the total count rate is calculated for the difference spectrum and compared with the statistical uncertainty of the measurement determined from the standard deviation in the rolling average background (σ_B) and poisson uncertainty in the difference spectrum count rate. A measure of significance, σ, is defined by the ratio of the total count rate in the difference spectrum ($\dot{N}_D$) to the uncertainty.

$$\sigma = \frac{\dot{N}_D}{\sqrt{\sigma_B^2 + N_D / t_m^2}}$$

Any spectrum where the difference spectrum count rate is within 3σ of the background is considered to be consistent with natural variation, and is accepted. Any measurement where this is greater than 6σ is considered to be significantly different from natural variation, and is rejected. These thresholds are based on an assumption that, in an environment with a slowly varying background, the difference spectrum count rate will follow an approximately normal distribution. Figure 1 shows histograms for the measure of significance for (a) laboratory measurements and (b) data collected over Cumbria in June 2000. Even in field measurements, the assumption of an approximately normal distribution around the rolling average is justified.

A further test is applied to the spectra between these limits, with the analysis above repeated for count rates for the spectral windows used in the standard windows stripping analysis. Any spectra where any of the measures of significance for these windows is greater than 3 are rejected.

If all these filters are passed, the current measurement is then added to the rolling average background, with the oldest spectrum in the background removed. This background is then subtracted from the next measurement, and the process repeated. On occasions, spectra that do not record a radiation anomaly will be rejected. However, as the rolling average background does not need to include all the local background measurements to be representative, this is not considered to be a significant loss of information.

The display of the difference spectrum is colour coded in a similar manner to conventional rainbow plots. In the SUERC software these colours run from dark blue (lowest) to red (highest). For the difference spectrum a threshold corresponding to no significant difference compared to the average background is applied, with all channels with magnitude less than this coloured white. Greens and blues indicate negative counts, with oranges and reds positive counts. This results in a simple method to identify spectra that differ from the local background, showing both the full energy peak and scattered radiation contribution to the spectrum. The scattered contribution is especially important if the source is shielded, not only can it reveal the presence of a strongly shielded source, it may be possible to determine some information about the shielding from this scattered component.

An event log, listing all the measurements that the filter determines to be a rapid change in the radiation field, and hence excludes from the rolling average background, is recorded. This includes the spectrum number, position and the measures of significance of the event for the total count and the largest single spectral

channel. This log is a list of measurements that could potentially indicate a point source, or other feature of interest, and warrant further analysis.

3. Case Studies

To illustrate this method, some data from past surveys have been analysed as though collected in real time.

3.1 Improved signal to background

The method described here calculates a rolling average background spectrum that can be subtracted from measured data. In environments with a large background, this method should suppress that in the difference spectra making a significant improvement in signal to background ratios for any sources in the area. During the 1995 Resume Exercise in Finland [11], a source search exercise included some ^{137}Cs sources in an area with significant levels of Chernobyl fallout (50-80 kBq m^{-2} of ^{137}Cs in 1995). Figure 2 shows the count rates, from 2s measurements, for the ^{137}Cs spectral window for a section of the survey produced using the spectral stripping method employed during the exercise and the differential approach described here using ten spectra in the filtered rolling average background. The data section includes a small lake (measurements 325-340) and a 2.8 GBq ^{137}Cs source passed three times at different distances (measurements 560, 680 and 720). The stripped count rate of 500-1000 cps due to Chernobyl fallout has been largely removed by the rolling average background subtraction.

3.2 Irish Sea Salt Marshes

Along the Irish Sea, salt marshes have accumulated radionuclides discharged from the Sellafield site since the 1950s, with ^{137}Cs being a prominent component of the radiation signals detected by AGS measurements over these features. These salt marshes vary considerably in extent, from several kilometres to just a few metres. In many cases, they also have clearly defined physical boundaries; some have embankments on the landward side, others have deep river channels on the seaward side. These features provide a set of good examples to illustrate the filtered differential background method.

Figure 3 shows spectra, with a 2s measurement time, collected crossing a small salt marsh feature (about 100x300m, with the flight lines perpendicular to the longer axis) in Cumbria in June 2000 [23], located approximately 9 km SSW of Kendal where the River Gilpin joins the River Kent forming a small sediment trap (grid reference SD475843). The feature shows enhanced levels of ^{137}Cs activity of about 50 kBq m^{-2}, with a total activity of 1-2 GBq. The full NaI spectra are shown, along with the differential spectra determined from backgrounds with and without filtering with 10 spectra in the local background. Figure 4 shows a set of rainbow plots for a small section of survey either side of this narrow feature (marked by the arrow). Approaching the salt marsh, the NaI spectra show a small peak due to ^{40}K at 1462 keV, with a smaller peak at 2614 keV from ^{208}Tl evident in the rainbow plot. The differential plots show this particular spectrum to have slightly more activity than the local backgrounds. As the aircraft passes over the salt marsh shows the ^{137}Cs peak

at 662 keV is evident in all the spectra. The differential spectra show a strong signal from ^{137}Cs without the natural activity, with the scattered component at lower energies resulting from the source burial clearly evident. After passing the feature, the differential spectra calculated without filtering the local background show a negative feature because the local background includes the ^{137}Cs activity on the salt marsh. The filtering removes this negative artefact.

Figure 4 also shows data over a more extensive feature south of the small feature shown in figure 3. The effect of reducing the difference spectra by not filtering the spectra included in the background is clear from this data. The rainbow plot for the unfiltered difference spectra shows an apparently much smaller feature, with a very distinct negative response afterwards. Filtering the spectra included in the background retains the full spatial dimensions of this salt marsh, and internal variation in the ^{137}Cs activity across the marsh.

As noted previously, the differential spectra reveal details of the scattered radiation contribution to the spectra. From this some details of the shielding of the source can be inferred. It can be seen on figure 3 that there is a strong scattered contribution from the ^{137}Cs on the salt marsh, which is a result of the burial of the active sediments by less active material reflecting the discharge history of Sellafield. The differential spectra can be used to estimate this source burial.

Figure 5 shows a spectrum recorded with a total 6 s integration time using a 16 litre NaI(Tl) detector at 50 m ground clearance, hovering over a calibration site on Caerlaverock Merse in Dumfries and Galloway in April 1999, with the average local

background determined using the filtering method described here subtracted. A ratio of the peak area (A) to the mean counts per channel of the valley (B_T) can be used to estimate the mean mass depth of the source (β). Previous work [24] with small NaI(Tl) detectors at 1 m height has shown that

$$\log \beta = 2.39 - 0.0346\left(\frac{A}{B_T}\right)$$

For larger airborne survey detectors it is expected that a similar relationship will hold, with the differences in peak to Compton ratio between detectors secondary to the scattering due to the soil and air path. To first order, the additional intervening air path for an airborne detector can be considered as an additional mass depth of 1.2 g cm^{-2} for every 10 m ground clearance. Full Monte Carlo simulation or extensive ground to air comparisons would be needed to precisely define the parameters for airborne detectors, but for illustrative purposes the relationship above is assumed to give an approximate value for the mean mass depth determined from such systems. For the spectrum shown in figure 5, A=1542±39 and B_T=51±3 giving an approximate mean mass depth β=22±3 g cm^{-2}, with a mean mass depth of approximately 16±3 g cm^{-2} after accounting for the 50 m air path. During the April 1999 survey [23], soil cores were collected from the calibration site. Analysis of these cores gives a mean mass depth on the calibration site of 17.1±1.2 g cm^{-2}.

The same approach can be taken to a larger data set. Figure 6 shows the distribution of ^{137}Cs mean mass depth across the Rockcliffe Marsh near Carlisle estimated from data collected in April 1999 [23], using 3s measurement times and 10 spectra in the filtered local background. The figure shows the expected distribution of shallower burial near the centre of the marsh, which is rarely inundated with a subsequent lower

sedimentation rate, and deeper burial near the fringes where the sedimentation rates are higher. A set of cores were collected across the central part of the merse in April 1999. The mean mass depth of the ^{137}Cs activity for these cores ranges between 8 and 12 g cm^{-2}, about 20% shallower than estimated by this analysis.

3.3 Source Search Exercises

In addition to identification of sources from a display of the difference spectra, the difference data can also be directly mapped to provide a means of rapidly locating such sources. Normally, such mapping would be accomplished using a traditional approach such as spectral windows method with stripping [1-3, 15] or principal component analyses such as NASVD [5, 25-26] or MNF [27]. The spectral windows method can be applied in real time, the principal component methods rely on the statistical properties of large data sets and so can only be used in post-survey analysis. As noted above, the spectral windows method depends upon some prior assumptions of the nuclides present in the environment and the level of shielding (eg: the depth profile of potentially buried activity). This, with the fact that the parameters for the windows method may be imprecisely determined prior to a survey, may result in some erroneous characterisation of the measured radiation field or even missing a source entirely. The filtered rolling average method presented here only assumes that the natural radiation field varies slowly, hence the difference spectra can be used to map signals without any other assumptions.

Figure 7 shows a plot of count rate for a window around the ^{60}Co peaks for a small data set collected during the 1995 Resume Exercise in Finland [19] using 2s

measurement times. The right hand map shows count rates for the ^{60}Co window from spectra following subtraction of a filtered rolling average background of 10 spectra. For comparison, the left hand map shows stripped count rates for this window following conventional analysis in 1995. This exercise included a source search with four ^{60}Co sources placed in the survey area in the positions marked. It can be seen that both methods locate three of the sources, the fourth source towards the south of the survey area was highly collimated and was not detected by any team participating in the exercise. Though, the difference spectra do generate a false positive and a very small signal for the most westerly of the sources.

3.4 Harwell and Rutherford Appleton Laboratories

In September 1996 an airborne survey was conducted of the former Greenham Common airfield, the town of Newbury and surrounding areas [28] using 3s measurement times for the NaI(Tl) detector. This survey included the area around the Harwell and Rutherford Appleton Laboratories. Around the perimeter of these sites, several strong signals were detected associated with activities within the site, including signals from machine sources and stored materials. In a follow up study in 1997 [29], rainbow plots were used to help identify the locations and nature of these features. Figure 8 shows rainbow plots for the data collected around the perimeter of these sites, for both the gross spectra and filtered differential spectra using 10 spectra in the local average background, with the features identified in the 1997 study indicated. It can be seen that the rainbow plots for both the gross and filtered difference spectra highlight a number of different features, although the filtered

differential is not indicating any features not originally identified from the gross spectra.

The event log file for this data set, containing a list of the spectra which were excluded from the rolling average background with their positions and a numerical indicator of the significance of the criteria on which they were excluded, was used to generate a map of the distribution of the measurements that differ significantly from the local background, shown in figure 9. The gamma ray dose rate distribution determined from the original analysis in 1996 is also shown.

These figures show a number of features that had been identified in the 1997 study. To the north of the site is the Liquid Effluent Treatment Plant (features N, Q and R) with signals due to ^{137}Cs and ^{60}Co. To the south of this are signals from the Tandem Van de Graaff accelerator (features A and F) with the distinctive machine source gamma ray distribution to energies above 3 MeV. To the southwest of the Tandem are further machine source signals associated with the ISIS and HELIOS accelerators, with some signals from ^{60}Co (features B, G and K). The remaining large signal to the north west of the site is from the B462 Active Handling Facility (features D, E, I, J, M and P) with signals due to stored Th ore and ^{137}Cs and ^{60}Co.

Extensive study of the data set in 1997 identified two smaller features. One was in the vicinity of the PLUTO reactor building to the south west of the site (features C, H and L), with the other to the south of the Tandem accelerator (feature O). The first of these is evident from the gamma dose map, and appears as a low significance signal in the event log map. The second is not clear in the dose rate map (where, it could easily be

additional shine from the accelerator) but is clearly visible in the map generated from the event log as an extended feature. Subsequent ground based measurements in 1997 identified this with the RAL sports field, and attributed the signal to soil imported for the field with higher natural activity levels than the local chalk [29]. These features, that required expert analysis to identify in 1997, would be clearly evident to a non-expert using the differential spectra and filtering log information generated by the approach outlined here.

4. Conclusions and Recommendations for Further Research

A method of visualising changing radiation environments that is well suited to real time identification of small sources in an environmental survey has been presented. This involves the calculation of a difference spectrum by the subtraction of a local background from each recorded spectrum. This local background is calculated from a rolling average of recent spectra. The use of a filter to exclude spectra that show signals significantly different than would be expected for slowly varying radiation fields has been described that removes effects, such as negative bounce-back following the leading edge of radiation features and false positive difference spectra after crossing a body of water. Unlike conventional approaches to real time data analysis, this method requires no prior knowledge about the distribution of activity in the survey area or detector calibration parameters.

The method retains the full spectral information, in contrast to similar rolling average background subtraction methods that use nuclide specific count rates. This includes

scattered components of the radiation field, which can be used to estimate the shielding around a given source as illustrated by a case study to estimate the source depth of activity buried on estuarine salt marshes, and radiation from machine sources or Bremsstrahlung from pure β emitting nuclides that does not exhibit a defined peak. The approach also allows for the identification of radionuclides that may not be included in standard processing. This method of determining and displaying difference spectra could prove very useful in real-time monitoring of gamma spectrometric data, aiding the identification of any anomalous radiation signals and as an addition to the methods available for locating point sources or mapping dispersed activity.

Applications where this technique could be useful include emergency mapping of contamination following a nuclear accident, and the detection and location of point sources. In particular, when initial response is by non-expert operators based on limited knowledge of the sources likely to be encountered, the simplicity of this approach for the operator could be a benefit. The graphical outputs allow the operator to observe both full-energy peaks and scattered radiation components that differ significantly from the local background. The event log identifies the location of such significant variations, and may be used to complement other methods of generating alarm levels.

There are some situations where a full spectral processing approach may be considered computationally too intensive. For some systems used to locate radioactive particles on beaches, a simple technique is preferred to full-spectrum processing for this reason [30]. The approach described here could be used to retain full-spectral

information at minimal computational cost. Another potential application of this approach is the detection of the edges of environmental compartments, such as boundaries between large bodies of water and land or edges of estuarine salt marshes. It is well established that some common geo-statistical tools, such as Kriging, can only be robustly applied within single environmental compartments [31-33]. An automated edge detection procedure that allows data from different environmental compartments to be separated could facilitate the wider use of some of these techniques for the analysis of data collected by mobile systems.

It is recognised that the approach outlined here will fail in some situations. For example, it is very likely to generate anomalies if there is a wide range of ground clearance in the survey or if the detector performance changes. Also, the technique is sensitive to any sudden change in the radiation environment, and may fail to properly account for surveys that cross geological boundaries. It may be necessary to consider some operational constraints including maintaining constant ground clearance and detector stability. Care should be taken to ensure that the filtering process is not started where the background is not representative of the survey area.

There is probably scope for modification of the filter to optimise it for different scenarios. More intelligent filters could also be considered, for example based on soft computing methods [34] such as fuzzy logic or computational intelligence. Three of the many approaches currently used in radiation measurements and remote sensing are outlined below, with references to example applications.

Artificial neural networks (ANNs) are mathematical models that consist of large numbers of processing elements in networks of weighted connections, and can represent any function by iteratively adjusting the network using sample data sets. The training process can be computationally intensive, but once trained ANNs can process data relatively rapidly. They are particularly appropriate for the analysis of highly dimensional or multivariate data such as gamma ray spectra due to their inherent parallel processing nature. ANNs have been used in a large range of filtering and classification tasks including portal monitoring [35], identification of radioactive contamination in air filter samples [36] and radionuclide identification in gamma ray spectra [36-38].

If a multivariate statistical model can be determined then the data can be analysed without prior training. The use of linguistic variables and fuzzy set theory is routine for the classification of multi-spectral remote sensing data [39], which contain a significant degree of uncertainty and imprecision.

A further approach commonly used in the analysis of remote sensing imagery is the naïve Bayes classification [40]. With multivariate data, naïve Bayes classifiers treat each variable as independent, and apply Bayes theorem, to derive probabilities for different hypotheses. Provided the correct classification is more probable than other classes, class probabilities do not need to be estimated precisely and the classifier is robust despite the underlying naïve independent variable model. Because independence between the variables is assumed, the entire covariance matrix does not need to be determined, and so a small training data set is sufficient.

The work described here uses a rolling average background that works linearly with time, averaging the most recent spectra recorded by the system. Spatial averaging, including spectra from nearby positions recorded on other flight lines as well as those on the current flight line, should increase the power of the method. This could be done in real time with the data set as recorded prior to that point in the survey, or post survey when the entire data set is available.

At present, the options of using soft computational methods to filter the rolling average background, or generating a spatially averaged background, have not been explored. Work is required to assess and implement the various options available. The method described here has, however, been shown to be a potentially useful tool for the visualisation of rapid changes in the radiation environment, and for processing gamma spectrometric data with limited assumptions about the radiation sources present.

References

[1] International Atomic Energy Agency, Airborne Gamma Ray Spectrometer Surveying. Technical Reports Series 323, IAEA, Vienna, 1991.

[2] International Atomic Energy Agency, Guidelines for Radioelement Mapping Using Gamma Ray Spectrometry Data. IAEA-TECDOC-1363, IAEA, Vienna, 2003.

[3] International Commission on Radiation Units and Measurements, Gamma-ray Spectrometry in the Environment, ICRU Report 53, ICRU, Bethesda USA, 1994.

[4] D.C.W. Sanderson, J.D. Allyson, A.N. Tyler, In: IAEA Technical Committee Meeting on the Use of Uranium Exploration Data and Techniques in Environmental Studies. IAEA-TECDOC-827, IAEA, Vienna, 1994, pp. 197-216.

[5] H.K. Aage, U. Korsbech, Appl. Radiat.Isot. 58 (2003), 103-113.

[6] D.G. Jones, P.D. Roberts, M.H. Strutt, J.J. Higgo, J.R. Davis, J. Environ. Radioact. 44 (1999), 159-189.

[7] L.J. Deal, J.F. Doyle, Z.G. Burson, P.K. Boyns, Health Phys. 23 (1972) 95-98.

[8] Q. Bristow, Current Research Part B Geological Survey of Canada Paper 78-1B (1978), 151-162.

[9] R.L. Grasty, In: K.B. Haley, L.D. Stone (Eds.), Search Theory and Applications, Plenum Publishing Corporation, New York, 1980, pp. 211-220.

[10] C. Marcos, F. Moreira, Health Phys. 60 (1991) 81-85.

[11] J. Hovgaard (Ed.), Rapid Environmental Surveying Using Mobile Equipment. ISBN 87-7893-014-6. Nordic Nuclear Safety Research, Copenhagen, 1997.

[12] S. Karlsson, H. Mellander, J. Lindgren, R. Finck, B. Lauritzen, RESUME 99: Rapid Environmental Surveying Using Mobile Equipment, NKS-15, ISBN 87-7893-065-0, NKS Secretariat, Roskilde, Denmark, 2000.

[13] Swedish Rescue Services Agency, Evaluation: Barents Rescue 2001, ISBN 91-7253-154-1, Swedish Rescue Services Agency, Karlstad, Sweden, 2002.

[14] T. Ulvsand, R. Finck, B. Lauritzen (Eds.), NKS/SRV Seminar on Barents Rescue 2001 LIVEX Gamma Search Cell, NKS-54, ISBN 87-7893-108-8, NKS Secretariat, Roskilde, Denmark, 2002.

[15] A.J. Cresswell, D.C.W. Sanderson, D.C. White, Appl. Radiat. Isot. 64 (2006) 247-253.

[16] B. Bucher, L. Rybach, G. Schwarz, Nucl. Instr. and Meth. A 540 (2005) 495-501.

[17] Ch. Bourgeois, L. Guillot, J.C. Broudieu, M. Mette, S. Gutierrez, D. Abt, H. Jannic, In: D.C.W. Sanderson, A.J. Cresswell, J.J. Lang (Eds.), An International Comparison of Airborne and Ground Based Gamma Spectrometry: Results of the ECCOMAGS 2002 Exercise held 24 May to 4 June 2002, Dumfries and Galloway, Scotland. ISBN 0-85261-783-6. University of Glasgow, Glasgow, 2003, pp. 207-220.

[18] D.C.W. Sanderson, A.J. Cresswell, I.M. Anthony, S. Murphy, In: D.C.W. Sanderson, A.J. Cresswell, J.J. Lang (Eds.), An International Comparison of Airborne and Ground Based Gamma Spectrometry: Results of the ECCOMAGS 2002 Exercise held 24 May to 4 June 2002, Dumfries and Galloway, Scotland. ISBN 0-85261-783-6. University of Glasgow, Glasgow, 2003, pp. 263-275.

[19] D.C.W. Sanderson, J.D. Allyson, P. McConville, S. Murphy, J. Smith, In: J. Hovgaard (Ed.), Rapid Environmental Surveying Using Mobile Equipment. ISBN 87-7893-014-6. Nordic Nuclear Safety Research, Copenhagen, 1997, pp. 237-253.

[20] T. Hjerpe, R.R. Finck, C. Samuelsson, Health Phys. 80 (2001), 563-570.

[21] T. Hjerpe, C. Samuelsson, C., Health Phys. 84 (2003), 203-211.

[22] K. Bargholz, F. Andersen, H.K. Aage, U. Korsbech, U, In: D.C.W. Sanderson, A.J. Cresswell, J.J. Lang (Eds.), An International Comparison of Airborne and Ground Based Gamma Spectrometry: Results of the ECCOMAGS 2002 Exercise held 24 May to 4 June 2002, Dumfries and Galloway, Scotland. ISBN 0-85261-783-6. University of Glasgow, Glasgow, 2003, pp. 221-240.

[23] D.C.W. Sanderson, A.J. Cresswell, D.C. White, S. Murphy, J. McLeod, Investigation of Spatial and Temporal Aspects of Airborne Gamma Spectrometry. Final Report. SURRC report for DETR (2001). DETR/RAS/01.001.

[24] A.N. Tyler, D.C.W Sanderson, E.M. Scott, E.M., J. Environ. Radioact. 33 (1996) 195-212.

[25] J. Hovgaard. Airborne Gamma-Ray Spectrometry. Statistical Analysis of Airborne Gamma-Ray Spectra. PhD Thesis, Technical University of Denmark (1997).

[26] H.K. Aage, U. Korsbech, K. Bargholz, J. Hovgaard, Appl. Radiat. Isot. 51 (1999) 651-662.

[27] B.L. Dickson, J. Environ. Radioact. 76 (2004) 225-236.

[28] D.C.W. Sanderson, J.D. Allyson, A.J. Cresswell, P. McConville, An Airborne and Vehicular Survey of Greenham Common, Newbury District and Surrounding Areas. SURRC Report for Newbury District Council, 1997.

[29] D.C.W. Sanderson, J.D. Allyson, A.J. Cresswell, An Investigation of Off-site Radiation Levels at Harwell and Rutherford Appleton Laboratory Following Airborne Gamma Spectrometry in 1996. SURRC Report for Vale of White Horse District Council, 1998 .

[30] M. Davies, G. McCulloch, I. Adsley, J. Radiol. Prot. 27 (2007) A51-A59.

[31] B.C. Hope, Exploring Advanced Methods for the Visualisation and Presentation of Aerial Gamma-ray Survey Data. MSc Dissertation, University of Glasgow, 1998.

[32] P. Krejčíř, An Estimator of the Radioactivity Inventory in Solway Firth and Ribble Estuary. PhD Thesis, Charles University, Prague, 1999.

[33] D.C. White, A Comparative Study of Visualized AGS data at Various Spatial Resolution and for Various Interpolation Algorithms. MSc Thesis, University of Glasgow, 2000.

[34] Y. Dote, S.J. Ovaska, Proc. IEEE 89 (2001) 1243-1265.

[35] L.J. Kangas, P.E. Keller, E.R. Siciliano, R.T. Kouzes, J.H. Ely, Nucl. Instr. and Meth. A 587 (2008), 398-412. doi: 10.1016/j.nima.2008.01.065

[36] P.E. Keller, L.J. Kangas, G.L. Troyer, R.T. Kouzes, S. Hashem, IEEE Trans. Nucl. Sci. 42 (1995) 709-715.

[37] R.E. Abdel-Aal, M.N. Al-Haddad, Nucl. Instr. and Meth. A 391 (1997) 275-288.

[38] E. Yoshida, K. Shizuma, S. Endo, T. Oka, Nucl. Instr. and Meth. A 484 (2002) 557-563.

[39] M. Fauvel, J. Chanussot, J.A. Benediktsson, IEEE Trans. Geosci. Remote Sensing 44 (2006) 2828-2838.

[40] S. Aksoy, K. Koperski, C. Tusk, G. Marchisio, J.C. Tilton, IEEE Trans. Geosci. Remote Sensing 43 (2005) 581-589.

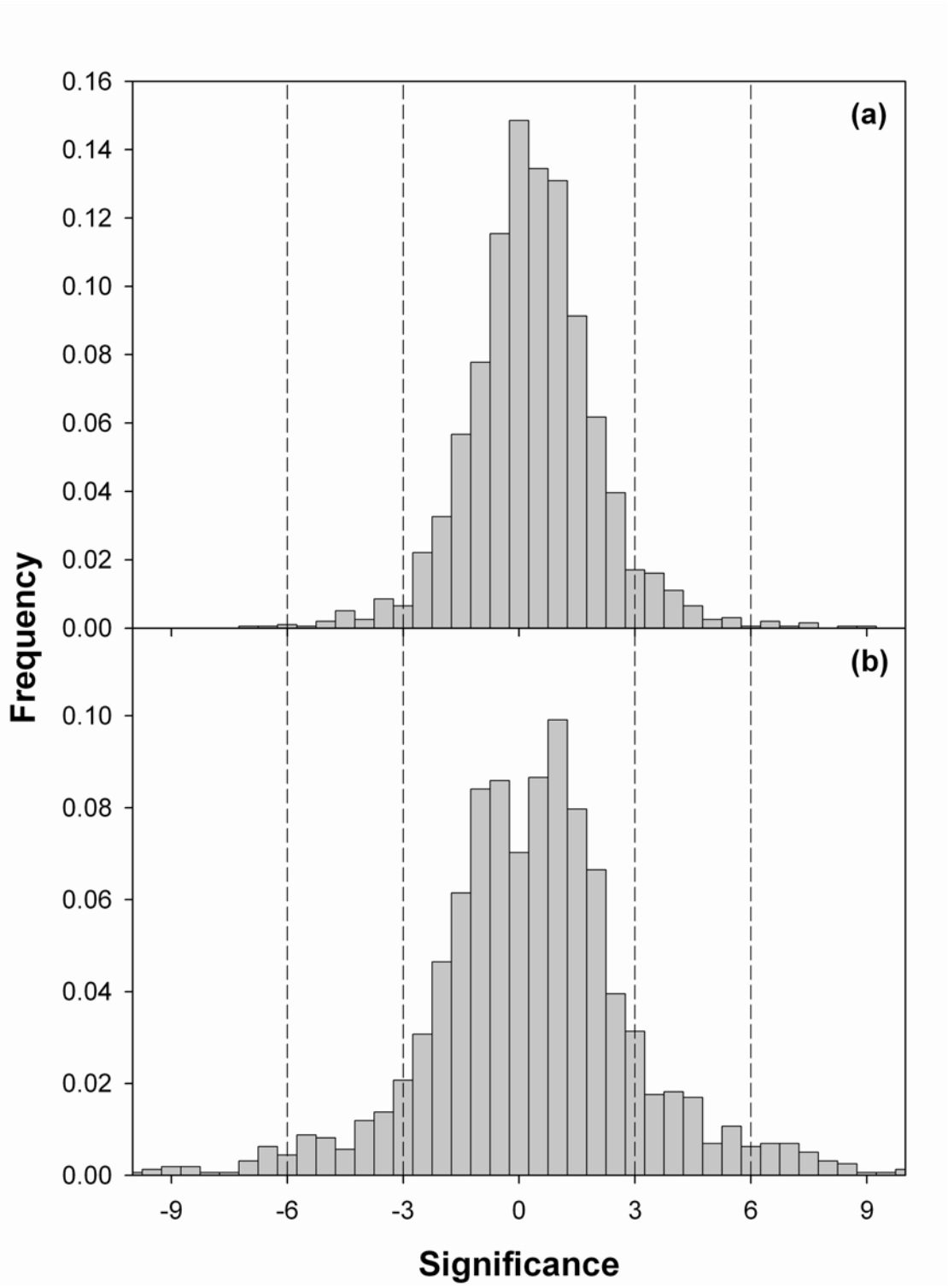

Figure 1: The distribution of the measure of significance for the total count rate, for data recorded (a) in the laboratory with a fixed detector and (b) during an airborne survey of Cumbria in June 2000.

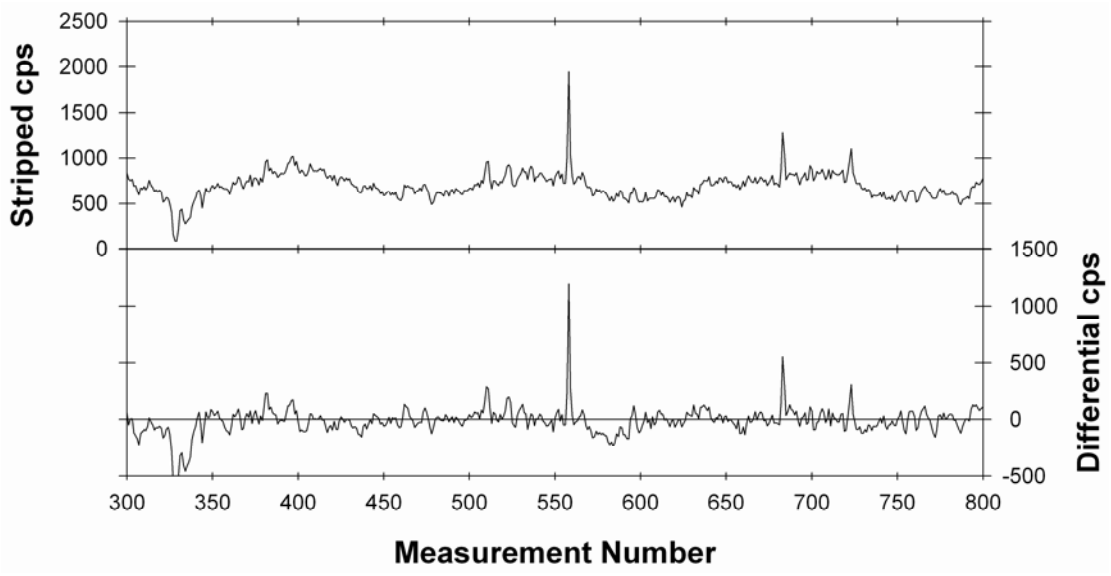

Figure 2: Count rates for the ^{137}Cs window determined using the spectral stripping method (top) and differential method described in this paper (bottom) for a section of a source search exercise in Finland in 1995. The profiles show a 2.8 GBq ^{137}Cs passed at different distances, a small lake and the Chernobyl fallout in the area in the stripped count rate suppressed by the rolling average background subtraction in the differential count rate.

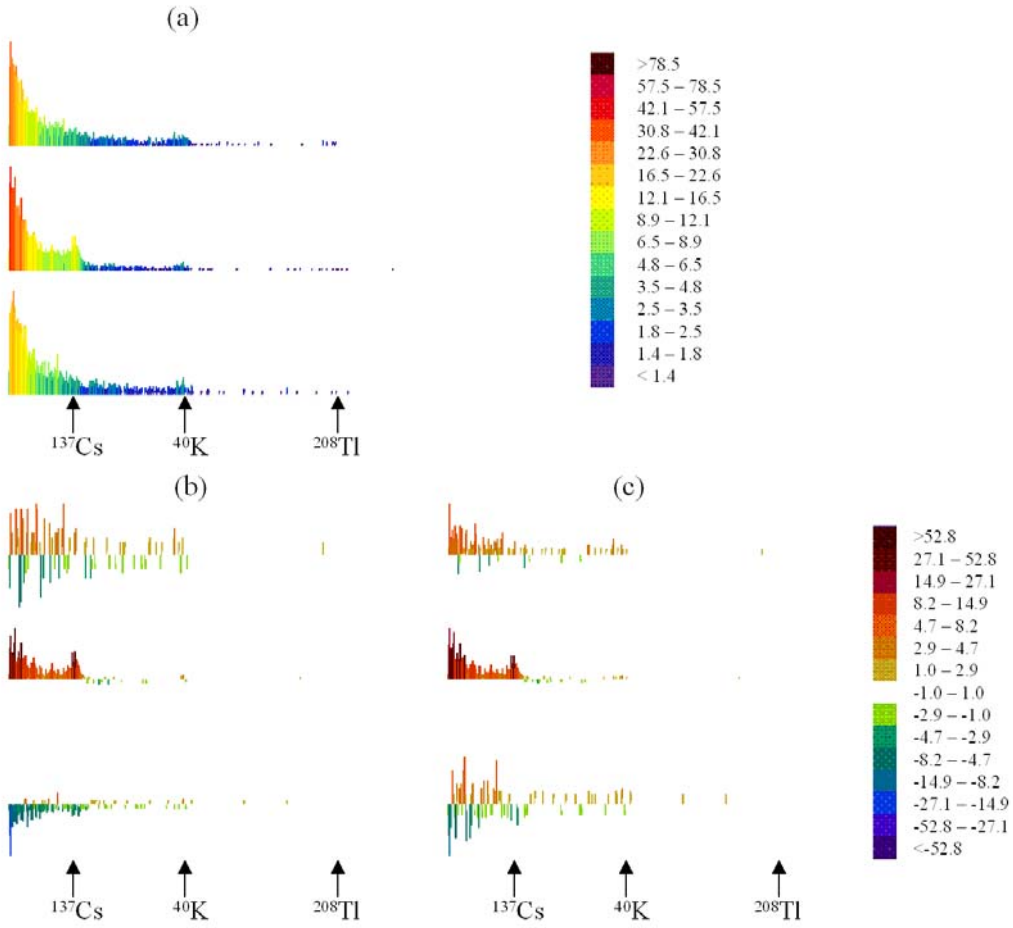

Figure 3: Spectra recorded using a 16 litre NaI(Tl) detector for a narrow feature in Cumbria, approaching from the north (top), crossing the feature (middle) and continuing to the south (bottom), with measurement positions approximately 200m apart. For the gross NaI(Tl) spectra (a) and difference spectra recorded without (b) and with (c) background filtering.

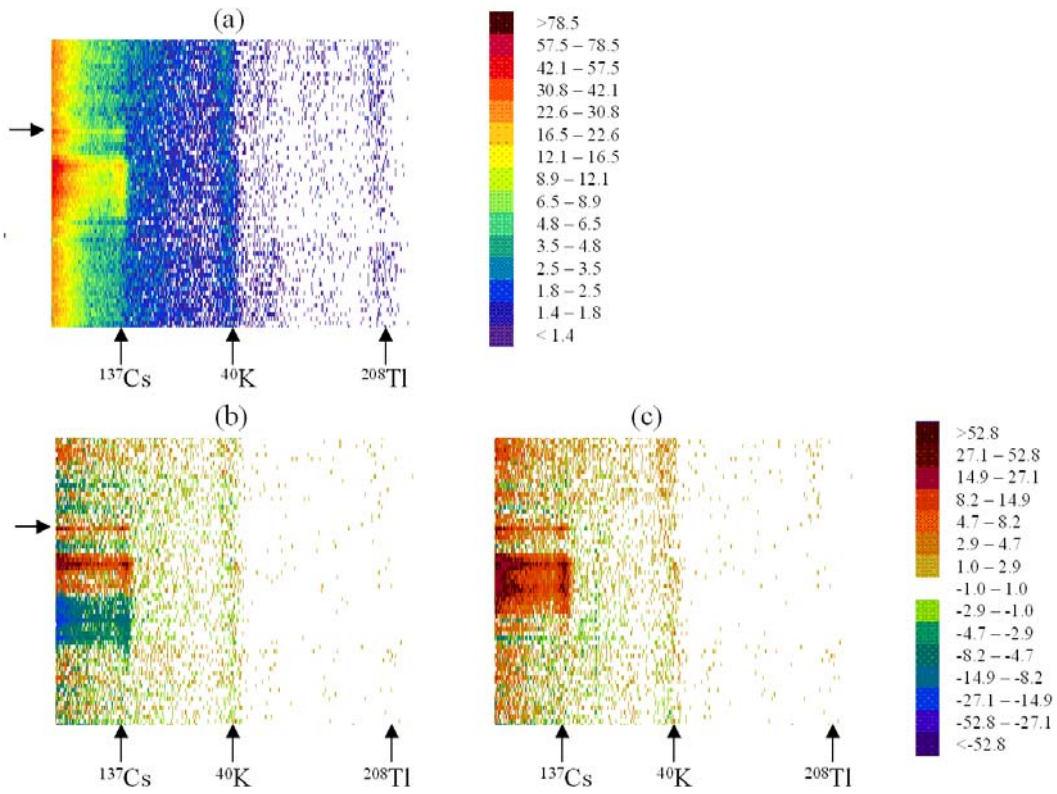

1

2 Figure 4: Rainbow plots for a 4 km long section of airborne survey in southern
3 Cumbria in June 2000, with the flight line direction from the north (top) to south
4 (bottom), for the NaI spectra (a) and difference spectra without (b) and with (c)
5 background filtering. The arrow indicates the narrow feature shown in figure 1.

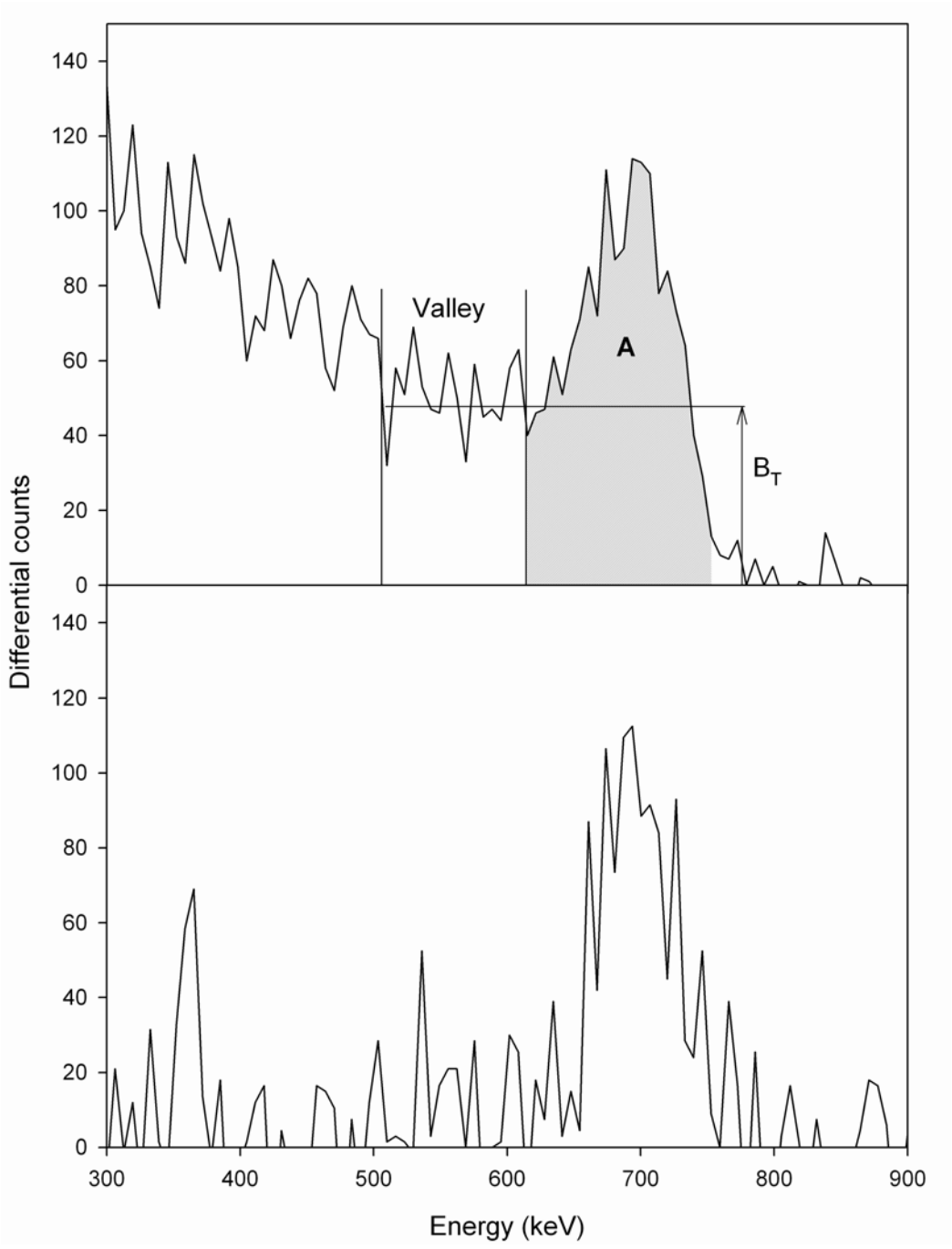

Figure 5: Spectrum recorded at 50 m above the Caerlaverock calibration site in April 1999 (top), using a 16 litre NaI(Tl) detector with a total of 6 s integration time and following subtraction of a filtered rolling average background. The peak (A) and valley (B_T) used to estimate source mean mass depth as defined in the text are shown. For comparison, a spectrum from a ^{137}Cs source in the laboratory with minimal scattering is also shown (bottom).

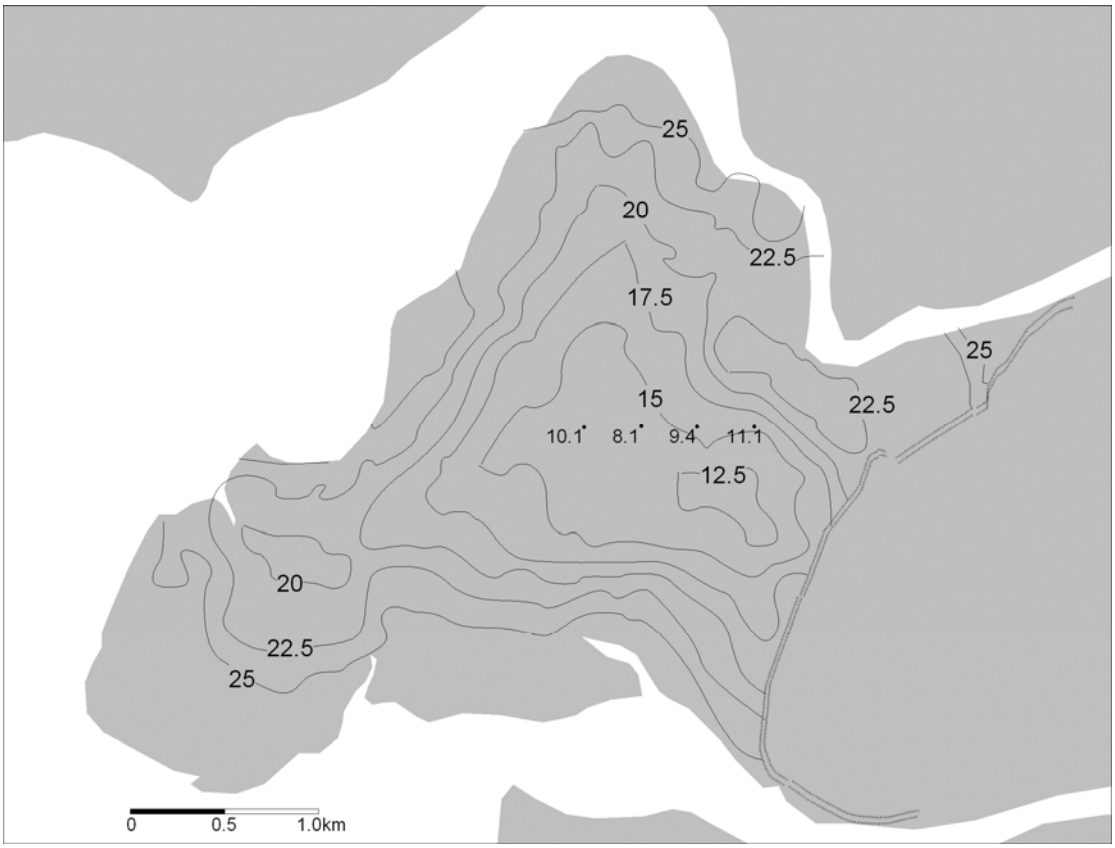

Figure 6: Mean mass depth (g cm^{-2}) for ^{137}Cs on Rockcliffe Marsh, estimated from difference spectra for the April 1999 survey data set. The locations of four cores collected at the time of the survey are also shown, with the mean mass depth determined for each core (uncertainties on the mass depths from the core data are approximately 8%).

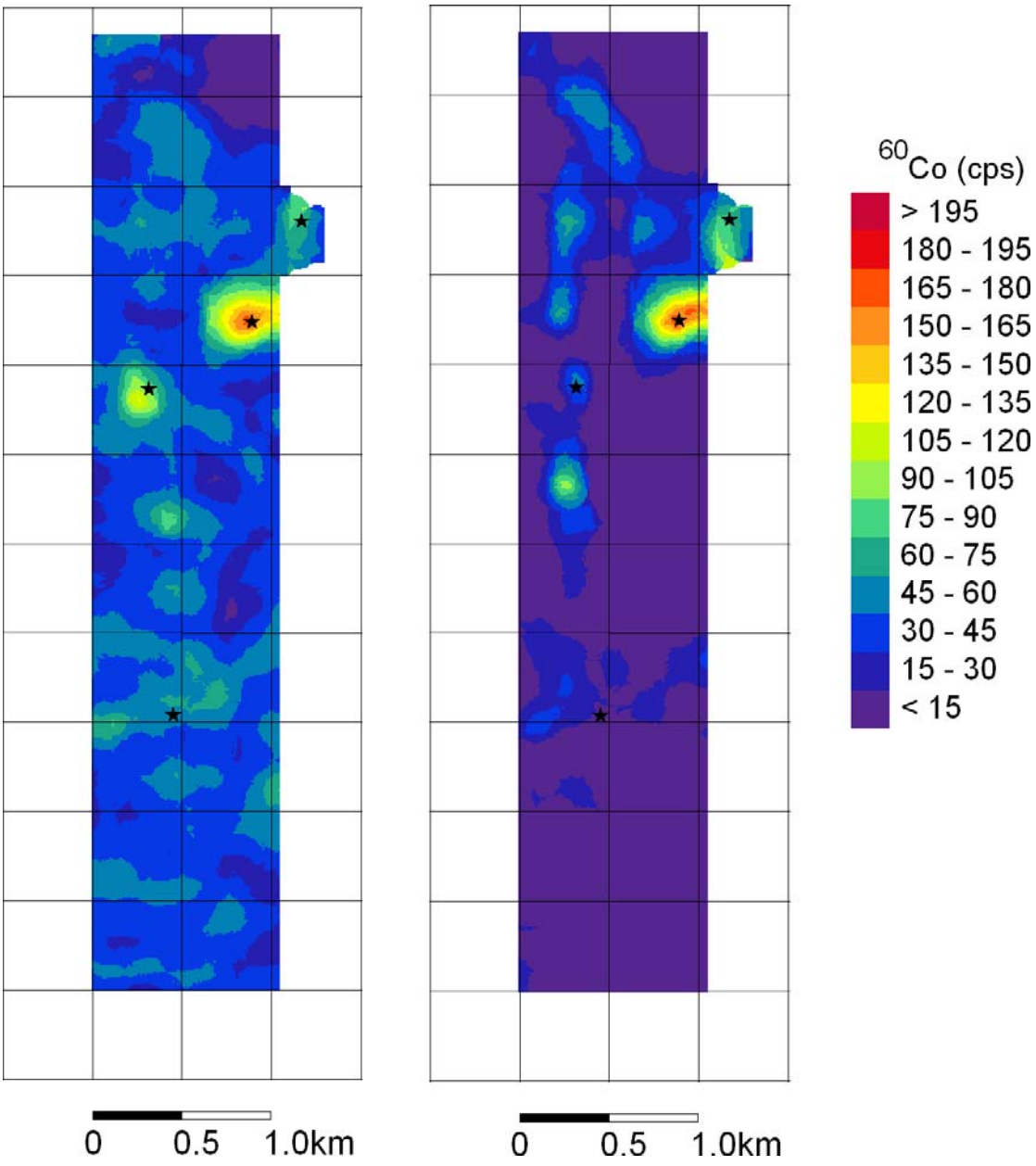

Figure 7: Count rates for a window around the ^{60}Co peaks for an area containing sources for the 1995 Resume Exercise, determined using conventional spectral stripping analysis (left) and after subtracting a filtered rolling average background (right). The locations of the four ^{60}Co sources are marked.

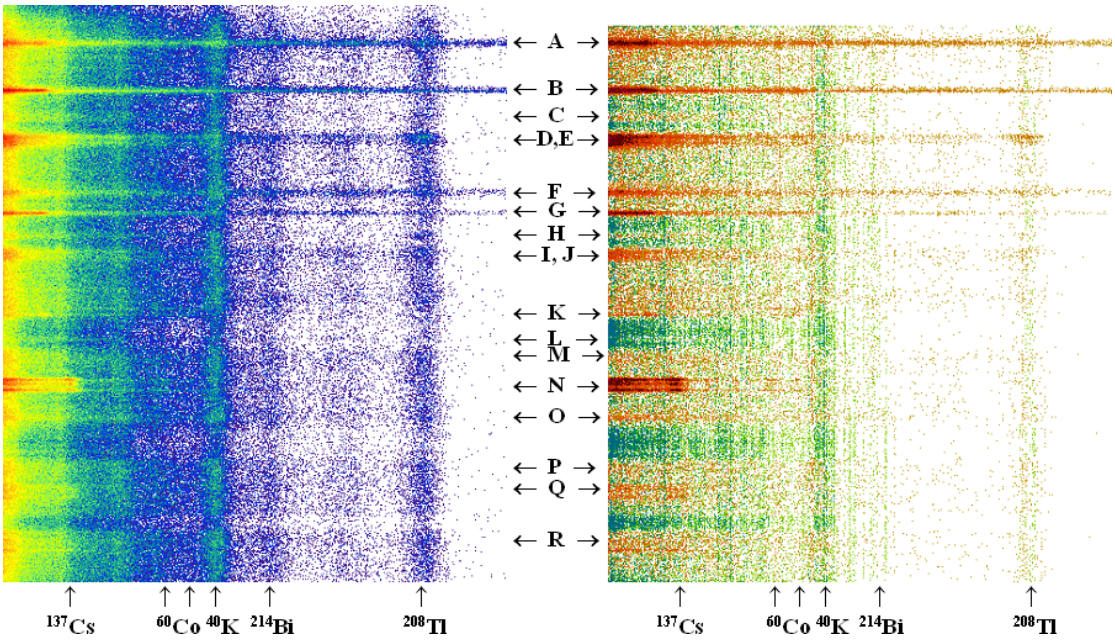

Figure 8: Rainbow plots for the gross spectra (left) and filtered difference spectra (right) from a series of circuits around the perimeter of the Harwell and Rutherford Appleton Laboratories in September 1996. Features identified in the earlier work [31] are indicated. Features N, Q and R correspond to the Liquid Effluent Plant to the north of the site; features A and F are from the Tandem Van de Graaff accelerator at the south east corner of the site; features B, G and K are from the ISIS and HELIOS accelerators towards the south of the site; features D, E, I, J, M and P are from the B462 Active Handling Facility at the north west of the site; features C, H and L are in the vicinity of the PLUTO reactor building at the south west of the site; and feature O is on the RAL sports field south of the Tandem.

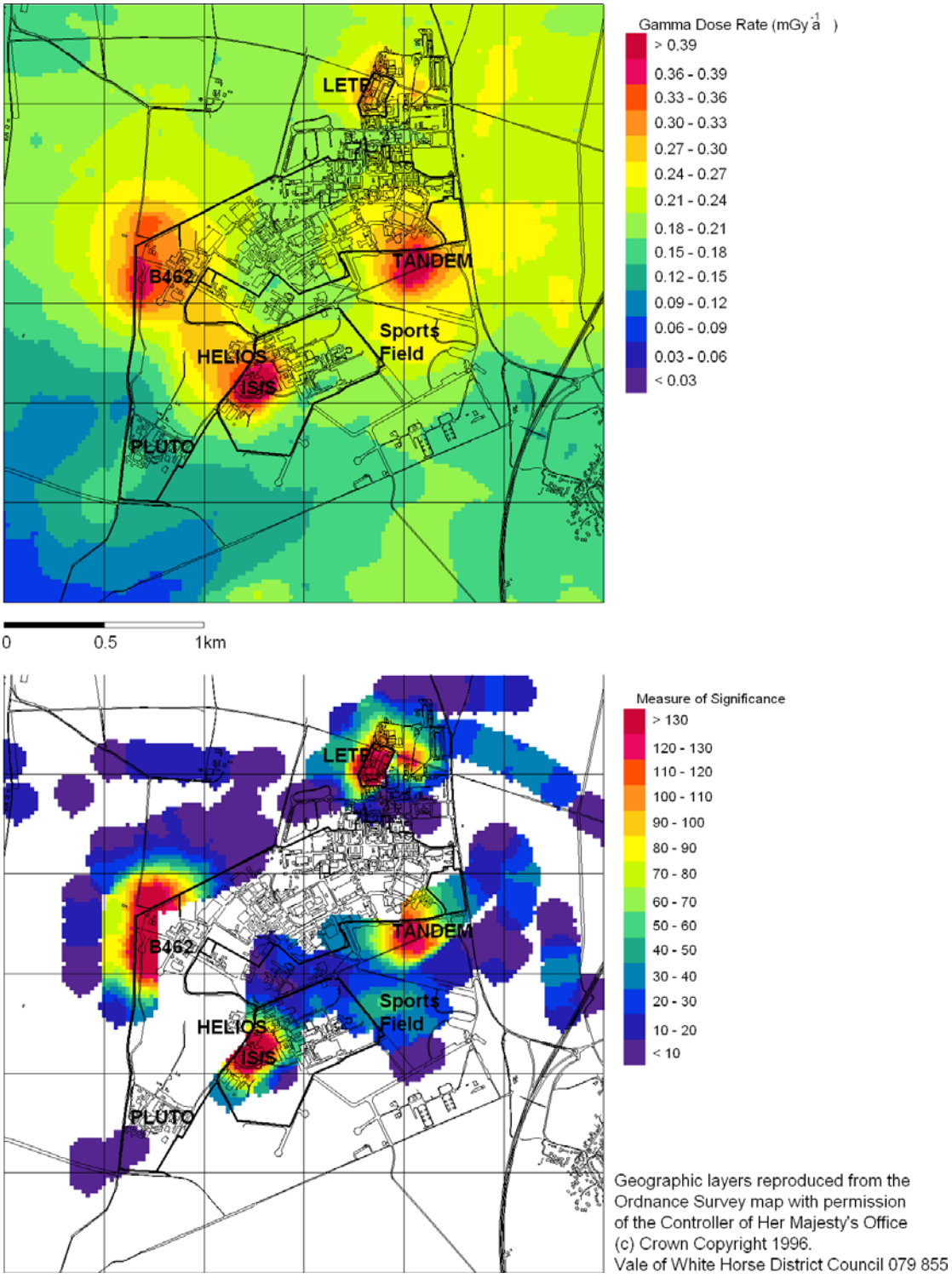

Figure 9: Maps of the gamma dose rate distribution (left) and events that trigger the filter (right) for the 1996 airborne survey of the Harwell and Rutherford Appleton Laboratories. The dose rate map is produced from approximately 900 measurements, the map of measurement of significance is produced from 260 measurements that triggered the filter.